Indian Journal of Science and Technology, Vol 9(39), DOI: 10.17485/ijst/2016/v9i39/102062, October 2016
ISSN (Print) : 0974-6846
ISSN (Online) : 0974-5645

Face Authentication System of Thermal Image with Gabor Filter

K. Annapurani*, C. Malathy, Hardeep Singh and Dhiraj J. Rathod

Department of Computer Science and Engineering, SRM University, Kattankulathur - 603203, Tamil Nadu, India; annapoorani.k@ktr.srmuniv.ac.in, malathy.c@ktr.srmuniv.ac.in, mannihardeep@gmail.com, veer.dheer@gmail.com

Abstract

Objectives: A new unique feature extraction technique for face authentication is implemented in thermal imaging. The proposed work extracts vasculature information creates a signature of thermal image and authenticates the individual. **Methods/Statistical Analysis**: A biometric system for face authentication with a better accuracy and reliability is proposed with an algorithm that uses morphological operators for feature extraction, Gabor filter for registration and correlation coefficient, similarity measures are used for matching. The operators used in image morphology are opening and top-hat segmentation. In order to ensure changes in vasculature at various time intervals four images are taken at different instants and thermal signature template is developed. Due to the consistent thermal features the biometric process is not affected. **Findings:** 22,784 images of eighteen subjects are used for testing the facial authentication system. An accuracy of 91% is obtained for skeletonised signatures using correlation coefficient which is better than Euclidean Distance that gives 88%. False Acceptance Rate (FAR) of the system is 0.0% for both Euclidean Distance and Correlation Coefficient. False Rejection Rate (FRR) of the system is 0.18% in the case of Correlation Coefficient and 0.24% in the case of Euclidean Distance. **Application/Improvements:** The enhancement of Face Authentication System to reduce the False Rejection Rate and improve the accuracy. The future scope of this work is the enhancement in military environment, where authentication is more important and the development of multimodal system.

Keywords: Authentication, Biometrics, Gabor Filter, Image Morphology, Image Registration, Thermal Imaging

1. Introduction

Biometric is the one which identifies or authenticates a person with the different traits or behavioural characteristics of human. The various traits as eye, ear, face, nose and so on or identifying individual biometrics is always a need in the field of biometrics; however the means of identification have changed considerably as populations have grown and developed technologically a lot. Biometric technologies have emerged as tools to help in the identification and authentication process. Most of the biometric systems consist of three elements: 1. Identity the person possesses (e.g. Social Security Number, Driver's License Number, Account Number), 2. Based on the status and location (e.g. Address, Profession, Education, Marital Status) and 3. Human body features and behaviour (fingerprint, voice, gait)[1].

The use of identifier possession, location and status was sufficient to verify a person but with huge population and technological growth, a robust identity management system is sought. It is the biometric system, recent biometric techniques strengthens the rapport with attributes and personal identifiers. More often it is possible to forge the personnel possession like identity cards and smart cards, but it is difficult to forge the personal features such as fingerprint, iris, ear, face and others.

Facial recognition[2] (or face recognition) is a process that can identify an individual by analysing and comparing patterns. The visible light portion of the Electromagnetic (EM) spectrum is used in this paper. Facial recognition systems are mainly used for identification purposes but are nowadays employed in a variety of other applications like entertainment, security, smart cards, passport, information security, law and medicine[3]. Face identification

*Author for correspondence

and face authentication are carried out in facial recognition system.

Identification is the claiming of an identity. A one-to-many comparison is done in the database as an attempt to establish the identity of a person not known is referred as identification. The identification system identifies an individual if the comparison of the sample to that of a stored template is within a threshold.

The process of verifying the claimed identity is known as authentication. Information Assurance (IA) has five components, out of which one is authentication. The other four are availability, integrity, non repudiation and confidentiality. In general authentication is done using the user name and passwords. If the password given is correct then that user is assumed to be authentic. Every user initially registers (or is registered by someone), using a self-declared or assigned password. Every time when the user logs in, he must know his password in order to access the system. But in biometric authentication it is enough that his trait is provided for verification, so that there is no need to remember the password. In authentication (or verification) mode a one-to-one comparison[4] of a biometric trait against his/her biometric feature stored as a biometric template is compared.

2. Related Works

Face recognition is the one that correlates the facial characteristics under and over the skin and the attributes such as eye, nose and portion of side faces and so on. Some of these characteristics vary with environmental factors (e.g. illumination), expressions (e.g. anger, happiness) and less permanency that can be altered. Different researchers have developed methodologies to address these problems. The work[5] represents face recognition based on physiological information; the characteristics under the skin are considered in this research.

In recent years, researchers have realized the potential of thermal Mid Wave Infra Red (MWIR) imagery for human identification using the vascular pattern extraction algorithm[6] for person verification applications. Also thermal images have been used to identify the affective state of humans[7].

Using visible and infra-red images comparison and combination of face recognition are performed[8]. In this paper the experiment in the time lapse between gallery and probe images are taken. Generally in face recognition, the challenge is the time–lapse scenarios. Visual and thermal image-based facial recognition adopts a feature selection technique and information fusion for improving accuracy[9]. The method employed in the paper[9] is modular Eigenspaces.

Many research works have been carried out in face recognition system and the performance[10] have been improved in the recent works. Major concerning performance factors are the difference in time between enrolment and acquisition of the unidentified facial image and the number of images required for each subject.

The work performed[11] in Facial Signature Authentication is extended by applying Gabor filters to images with various scales and orientations. The face variations are found by splitting the images into tiny modules that localises the facial variations. Section 3 discusses about the design of the system and Section 4 reviews the performance metrics.

3. Face Authentication System Design

There are many methodologies, algorithms and techniques adopted in the face recognition system using cameras in visible spectrum. But the use of thermal MWIR portion of the EM spectrum solves the problem of light variability[12]. Based on the different temperature range the false objects such as fake nose are detected. Even though more benefits are there for facial recognition system using MWIR, due to the high cost of cameras in MWIR than the visible counterparts MWIR face recognition system is still under research.

The proposed work extracts the features in the thermal image, produces templates from these features and compares the acquired features with the template through correlation coefficient and Euclidean method for authentication. The Figure 1 shows the different modules of facial system. The five major modules are:

- Data Collection.
- Registration of thermal infrared image.
- Thermal signature generation.
- Generation of thermal infra red template.
- Template and Signature Matching.

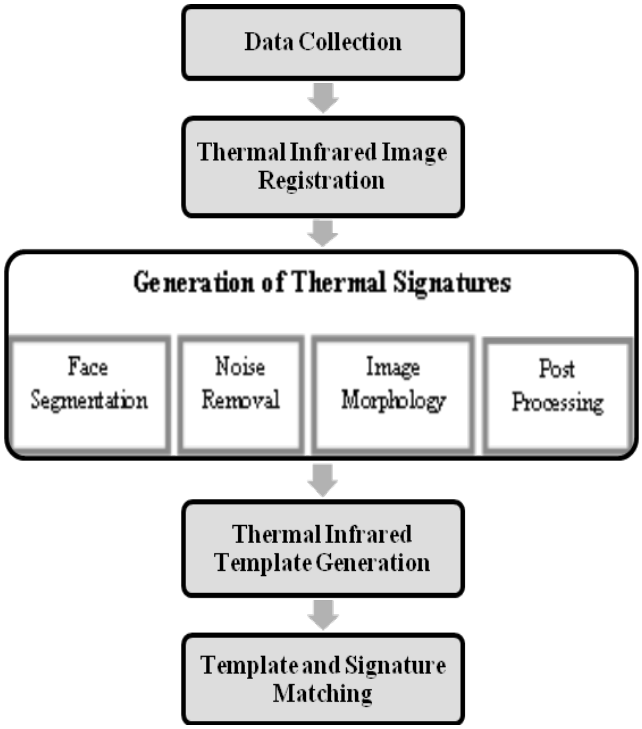

Figure 1. Flowchart of the thermal image face recognition system.

3.1 Data Collection

Collection of data was done using the online source http://www.vcipl.okstate.edu/otcbvs/bench/Data/04/download.html. In this paper, 22,784 thermal infrared images of 18 different subjects are used. These collected images are stored in a database named Datasets. Each subject is stored in the database with unique subject ID and names. Thermal images of the subjects are taken in different postures considering both outdoor and indoor environment as shown in Figure 2.

3.2 Registration of Thermal Infrared Image

Main task in the image processing field is image registration[13–19]. Different techniques are available for image registration of medical images and images in biometric

(a) (b) (c)

(d) (e) (f)

Figure 2. Thermal images of the subjects in different postures: (a) Indoor and (b) Outdoor environment, (c) Right and (d) Left neck movements, (e) Subjects with specks and (f) Hat.

applications. The process of feature extraction is carried out using Gabor filter.

In image processing, for edge detection a linear filter, Gabor filter is used. Gabor filter is especially used for texture representation and discrimination. In the spatial domain, a 2D Gabor filter is a Gaussian kernel function modulated by a sinusoidal plane wave. Representing orthogonal directions the filter has real and imaginary parts. The two components may be formed of a complex number are used individually. Its real component $g(x, y)$ $g(x, y)$ is represented by Equation (1) the filter has real and imaginary parts,

$$y; \lambda, \theta, \psi, \sigma, \gamma) = exp\left(-\frac{x'^2 + \gamma^2 y'^2}{2\sigma^2}\right)\cos\left(2\pi\frac{x'}{\lambda} + \psi\right) \quad (1)$$

Where

$$\mathbf{x}' = \mathbf{x}\cos\theta + y\sin\theta$$

and

$$\mathbf{y}' = -\mathbf{x}\sin\theta + y\cos\theta$$

In this Equation, λ represents the wavelength of the sinusoidal factor, θ describes the orientation, Ψ the phase offset, σ the standard deviation and γ the spatial aspect ratio.

During registration process from each subject four images are captured and one of the images are considered as the reference image. The flow diagram of the registration process is represented in Figure 3.

The thermal images are captured at different time intervals and change in the position of subjects with respect to the camera position. Because of this during data collection if there is any shift of position from the subject is there, it does not affect the registration process. Overlay of the signatures and templates are simplified and similarity measures are incorporated. Figure 4 shows the results of the registration process for one of the subjects.

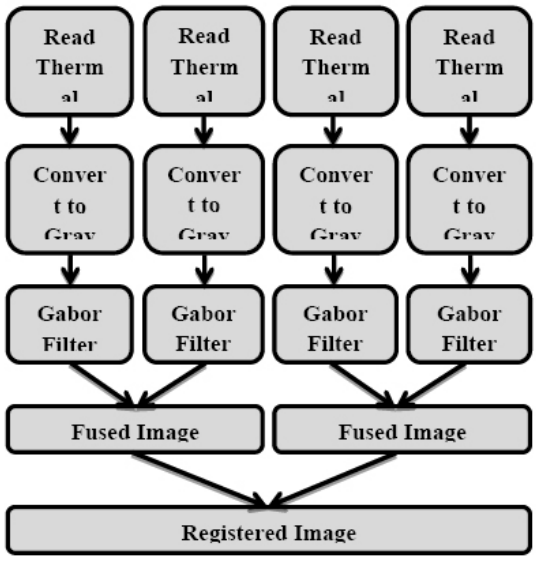

Figure 3. Registration process flow.

(a) (b)

Figure 4. Results of thermal image registration procedure. (a) Original thermal image (b) Registered image.

3.3 Generation of Thermal Signatures

Thermal signature from each subject was extracted and the signature process consists of four Sections. They are segmentation, noise removal, image morphology and post processing. Figure 5 displays the thermal signature generation process.

3.3.1 Face Segmentation

Localizing region-based active contours[20,21] is the technique used for segmenting the face, which uses non-homogeneous backgrounds and foregrounds. An initial contour is selected around the face to segment using contouring algorithm to a neighbourhood. Neck of the person is not considered in the face region segmentation. Let the closed contour of interest be c = {x| $\varphi(x)$ =0}. The closed contour C is expressed by the following approximation of the smoothed Heaviside function as given in Equation (2).

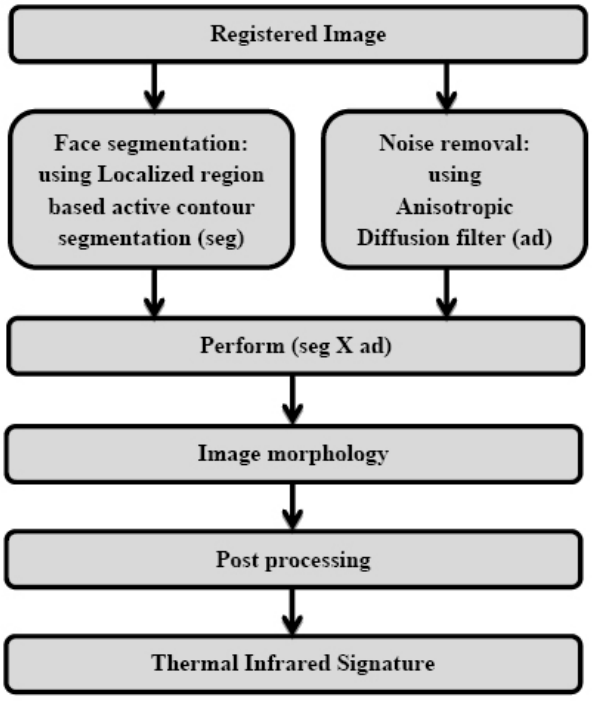

Figure 5. Thermal signatures generation flow diagram.

$$H\varphi(x) = \begin{cases} 1, & \varphi(x) < -\varepsilon \\ 0, & \varphi(x) > \varepsilon \\ \frac{1}{2}\left\{1 + \frac{\varphi}{\varepsilon} + \frac{1}{\pi}\sin\frac{\pi\varphi(x)}{x}\right\}, & otherwise \end{cases} \quad (2)$$

Where $\varphi(x)$ a contour and $[-\varepsilon, \varepsilon]$ represents the Heaviside function boundary. Similarly, the exterior of C is defined as $(1 - H\varphi(x))$.

The well-known Yezzi energy is used[22] in the energies of the exterior and interior contours for face segmentation. Figure 6(a) shows the resultant image after the segmentation procedure.

3.3.2 Noise Removal

After the face segmentation from the thermal infrared image, the noise signals are removed to improve the image for next stage of processing. A standard Perona–Malik anisotropic diffusion filter[23] is first applied to the thermal image. Anisotropic diffusion is the technique that reduces the noise in the images.

A 2D structure of network with 8 neighbouring nodes is taken for diffusion conduction. The neighbours considered are the east, west, north, south, southeast, southwest, northeast and northwest. The conduction coefficient function is used for the filter to enhance the regions of thermal

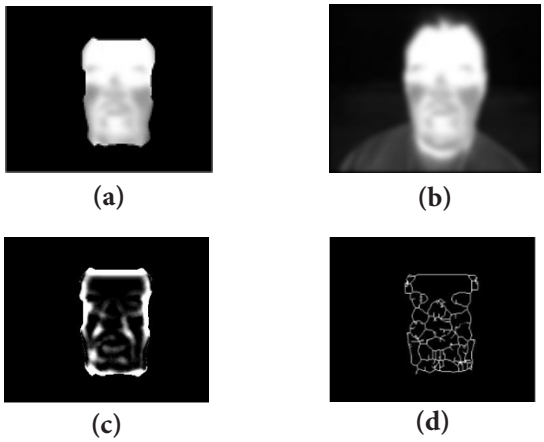

Figure 6. Thermal Signatures process (a) Face segmented image, (b) Anisotropic Diffused image, (c) Top- Hat segmented image, (d) Thermal signature.

conductivity incorporated with thermal signature. The function of conduction coefficient $C(x,y,t)C(x,y,t)$ is given by Equation (3);

$$C(x,y,t) = \frac{1}{1+\left(\frac{\|\nabla I\|}{K}\right)^2} \quad (3)$$

For the eight directions ∇I and the gradient modulus threshold K that controls the conduction are calculated.

Iterative process of anisotropic diffusion filtering is performed till a satisfactory smoothing is implemented, in this process ten iterations are used. Figure 6(b) shows the resultant image after the anisotropic diffusion process.

3.3.3 Image Morphology

Analysing images based on shapes are known as image morphology. Opening and top-hat segmentation are the operators used in this paper. An operation of opening is executed to maintain foreground regions that have a similar shape to the structuring element. In morphology, opening means the dilation of the erosion of an image I by a structuring element S as in Equation (4);

$$I_{Open} = (I \ominus S) \oplus S \quad (4)$$

Where I and I_{open} are the face segmented and the opened image respectively; $\ominus$ and $\oplus$ are the morphological erosion and dilation operators.

Top-hat segmentation is of two types. They are white and black top-hat segmentation. The bias between the input image and its opening by some structuring element is known as white top hat segmentation; the difference between the closing and the input image is referred as black top hat segmentation; in this work, white top-hat segmentation was performed as it does the enhancement of intense objects in the image. The selection of the top-hat segmentation is to segment the regions of higher intensity that demarks the facial thermal signature. It results in the enhancement of image in the maxima. Figure 6(c) shows the resultant top-hat segmented image. The I_{top} top-hat segmented image $_{is}$ given by Equation (5);

$$I_{top}=I-I_{open} \quad (5)$$

3.3.4 Post Processing

After obtaining the maxima of the image it is skeletonized. Skeletonization is a process of reducing foreground regions in an image to a skeletal remnant preserving the connectivity of the original regions.

Morphological thinning in a binary template is a miss- or- hit transformation. It is carried out in template matching where a series of templates from $L1 - L8$ are searched in the whole image. If the compared image is not in the template then there is a miss result that is represented as 0 otherwise as 1. Skeltonization of the image I_{skel} is given by Equation (6);

$$I_{skel} = (I_{top} / I_{top} \hat{x} L_i) \quad (6)$$

Where $\hat{x}$ is the miss-or-hit operator and L_i is the structuring elements set from $L1 - L8$. The structuring elements first two L1 and L2 are used for the skeletonization process are given in Equation (7);

$$L1 = \begin{bmatrix} 1 & 1 & 1 \\ 0 & 1 & 0 \\ 0 & 0 & 0 \end{bmatrix} \quad L2 = \begin{bmatrix} 0 & 1 & 0 \\ 0 & 1 & 1 \\ 0 & 0 & 0 \end{bmatrix} \quad (7)$$

The other six structuring elements was obtained by rotating both $L1$ and $L2$ masks by 90°, 180° and 270°. Figure 6(d) shows the final thermal signature.

3.4 Thermal Signatures Generation

Thermal signatures in any person varies slightly daily for various reasons like environmental temperature, weight, exercise, health of the subject, temperature of the imaging room and many more[24].

Due to these variations in our work we have developed a technique that gives the thermal signature template that preserves the significant features in a person's thermal sig-

nature over certain period. Figure 7 displays the flowchart of the entire template generation procedure.

Thermal signature template is generated by adding all the four thermal signatures extracted from individual's at slightly varying positions. It is done so to retain the considerable features from the subject. After that the resultant image is applied to the anisotropic filter to obtain the predominant features.

The generation of thermal signature template is illustrated in Figure 8. During testing process, a database of the templates is compared against any newly acquired thermal signature image.

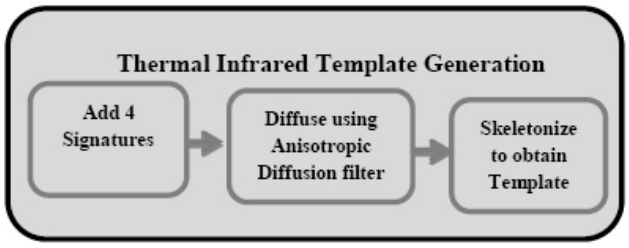

Figure 7. Template generation flow diagram.

(a) (b) (c)

Figure 8. Generation of thermal signature template: (a) Resultant image of addition of four thermal signatures, (b) Results of applying anisotropic diffusion on summed image, (c) Thermal signature template of the subject.

3.5 Template and Signature Matching

Matching as the name indicates a person or thing that equals or resembles another in some respect. Similarity measures[25] are widely used in applications like image databases that give the degree of closeness of query image to that of the gallery image. Similarity measures finds whether the thermal infrared template similar to that of the query thermal infrared signature.

3.5.1 Euclidean Distance

The distance between two pixels is calculated using Hamming distance, Euclidean Distance, Manhattan distance. In this paper, we have used Euclidean Distance method. The Euclidean Distance d is given in Equation (8).

$$d(p,q) = \sqrt{\sum_{i=1}^{n} (\dot{p} - \dot{q})^2} \quad (8)$$

Where, n is the number of dimensions and i ranges from 1 to n. It evaluates the difference for each corresponding attributes of pixel p and pixel q. Then the summation of square of differences in each dimension is calculated into an overall distance. Table 1 represents the results of Signature and Template matching using Euclidean Distance.

3.5.2 Correlation Coefficient

Based on the correlation coefficient, the closeness between two datasets can be found, the range of correlation coefficient is -1 to 1. If the two objects are perfectly related then the correlation coefficient is 1, which is positive correlation. If it is -1 then also it is correlated but in an opposite

Table 1. Signature and Template Matching using Euclidean Distance

	Sub01	Sub02	Sub03	Sub04	Sub05	Sub06	Sub07	Sub08	Sub09	Sub10
Sub01	0	134.58826	282.70479	297.59704	158.92136	288.36435	194.96666	200.92287	242.68498	119.84156
Sub02	134.58826	0	241.18872	239.13176	190.98167	195.33561	121.95081	122.89019	236.5333	118.76026
Sub03	282.70479	241.18872	0	68.264193	271.66524	159.20427	181.55991	195.90304	201.75232	307.66215
Sub04	297.59704	239.13176	68.264193	0	299.36266	130.19985	164.35936	189.05026	205.62587	312.58919
Sub05	158.92136	190.98167	271.66524	299.36266	0	273.81746	249.85596	256.99416	325.79748	230.1304
Sub06	288.36435	195.33561	159.20427	130.19985	273.81746	0	159.73102	186.3384	267.49579	292.83101
Sub07	197.96666	121.95081	181.55991	164.35936	249.85596	159.73102	0	68.132224	169.61722	193.16314
Sub08	200.92287	122.89019	195.90304	189.05026	256.99416	186.3384	68.132224	0	161.22035	179.00279
Sub09	242.68498	236.5333	201.75232	205.62587	325.79748	267.49579	169.61722	161.22035	0	239.09412
Sub10	119.84156	118.76026	307.66215	312.58919	230.1304	292.83101	193.16314	179.00279	239.09412	0

way, which is negative correlation. If the correlation coefficient is 0, then they are not correlated. Correlation $corr$ is given by the following Equation (9).

$$corr(x,y) = \frac{\text{cov}\,ariance(x,y)}{s\tan darddeviation(x) \times s\tan darddeviation(y)} \quad (9)$$

Where, x and y represent two data objects. Table 2 shows the results of Signature and Template matching using Correlation Coefficient.

Here the correlation coefficient is used because its range lies from -1 to 1 compared to the Euclidean Distance whose range lies in power of 10's. As the correlation coefficient provides low range values it was easy to find the threshold value. In this case calculated threshold value is 0.9. So if the correlation coefficient value is greater than 0.9 then the subject is authenticated else if the correlation coefficient value is less than 0.9 then the subject is rejected.

4. Performance Metrics

The performance of face authentication system is analysed using False Acceptance Rate (FAR), the False Rejection Rate (FRR), Equal Error Rate (EER) and Accuracy. When using a biometric application for the first time the user needs to enrol to the system. The system requests the face biometric from the user; this input is enrolled in the database as a template against his/her user ID. During verification process the user's acquired face biometric is compared with that of the template. If the query feature matches with the enrolled feature then the person is authentic otherwise not. This matching process is done using the correlation coefficient algorithm and the Euclidean method.

FAR is the probability that non-genuine users are authorised, due to incorrect matching of the biometric input with the stored template. It is also known as the type II error. FAR is defined as in Equation (10);

$$FAR = \frac{numberoffalseaccep\tan e}{numberofidentificationattempts} \quad (10)$$

Out of 20,000 identification attempts; number of false acceptance of the subject was 0 in both Euclidean Distance and Correlation Coefficient. So FAR of the system is 0.0% for both Euclidean Distance and Correlation Coefficient. Figure 9 represents the FAR of the system using both Euclidean Distance and Correlation Coefficient.

FRR is the probability that the genuine users are incorrectly rejected access to the system, due to wrong matching of the biometric input with a template. It is known as the type I error. A system's FRR is defined as in Equation (11);

$$\mathbf{FRR} = \frac{number\ of\ false\ rejections}{number\ of\ identification\ attempts} \quad (11)$$

Out of 2000 identification attempts; number of false rejection of the subject was 360 in the case of Correlation Coefficient and 480 in the case of Euclidean Distance. So FRR of the system is 0.18% in the case of Correlation Coefficient and 0.24% in the case of Euclidean Distance. Figure 10 represents the FRR of the system using both Euclidean Distance and Correlation Coefficient.

Table 2. Signature and Template Matching using Correlation Coefficient

	Sub01	Sub02	Sub03	Sub04	Sub05	Sub06	Sub07	Sub08	Sub09	Sub10
Sub01	1	0.6790098	0.7226314	0.7707511	0.4087632	0.6988455	0.3783522	0.3247501	0.4268662	0.2600945
Sub02	0.6790098	1	0.7084341	0.7473268	0.4023591	0.7861175	0.5210958	0.3983951	0.3265476	0.3478543
Sub03	0.7226314	0.7084341	1	0.7805793	0.4673991	0.685888	0.3247469	0.3212624	0.4106364	0.2531334
Sub04	0.7707511	0.7473268	0.7805793	1	0.4746204	0.78029	0.4473469	0.3245569	0.4136944	0.2689194
Sub05	0.4087632	0.4023591	0.4673991	0.4746204	1	0.4782538	0.4084556	0.4410029	0.2775775	0.245073
Sub06	0.6988455	0.7861175	0.685888	0.78029	0.4782538	1	0.4944281	0.4564298	0.3236127	0.353142
Sub07	0.3783522	0.5210958	0.3247469	0.4473469	0.4084556	0.4944281	1	0.5951238	0.3352935	0.3831275
Sub08	0.3247501	0.3983951	0.3212624	0.3245569	0.4410029	0.4564298	0.5951238	1	0.5135745	0.5073065
Sub09	0.4268662	0.3265476	0.4106364	0.4136944	0.2775775	0.3236127	0.3352935	0.5135745	1	0.48759
Sub10	0.2600945	0.3478543	0.2531334	0.2689194	0.245073	0.353142	0.3831275	0.5073065	0.48759	1

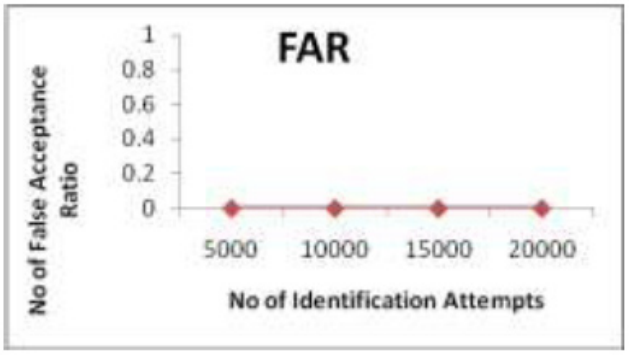

Figure 9. FAR of the system using both Euclidean Distance and Correlation Coefficient.

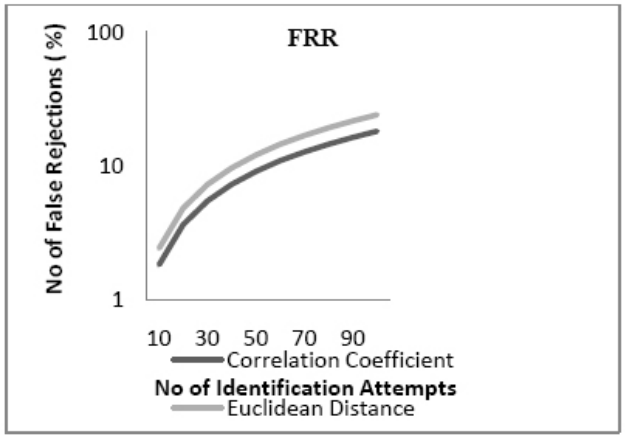

Figure 10. FRR of the system using both Euclidean Distance and Correlation Coefficient.

Equal Error Rate (EER) is the one where FAR and FRR are equal. The plot between FAR and FRR gives the EER curve. Accuracy of biometric systems is stated as in Equation (12);

$$Accuracy = 100 - \left(\frac{FAR + FRR}{2} \right)\% \qquad (12)$$

Results obtained for accuracy in the case of Correlation coefficient was 91% and in the case of Euclidean Distance was 88%.

5. Conclusions and Future Work

The proposed work was a new approach to biometric facial recognition based on extraction of features from different infrared thermal images. Gabor filter was used for thermal image registration and to segment the subject's face localized-contouring algorithms was used. Thermal signatures are created by morphological technique. Then signature template was created and matching process carried out. The matching between signatures and templates was done using a similarity measure based on; 1. The Euclidean Distance and 2. The Correlation Coefficient. The efficiency of the system is more by using the Correlation Coefficient when compared to the results using the Euclidian Distance. The results obtained in the matching process 91% in Correlation Coefficient and 88% in Euclidean Distance along with the generalized design process clearly demonstrate the ability of the thermal infrared system to be used on other thermal imaging-based systems and their related databases.

Further development of Face Authentication System is to reduce the False Rejection Rate and increase the accuracy of the system. It can also be further used in military applications to ensure the security of the system.

6. References

1. Pakutharivu P, Srinath MV. Comprehensive survey on fingerprint recognition systems. Indian Journal of Science and Technology. 2015; 8(35):2652–8.
2. Zhao W, Chellappa R, Phillips PJ, Rosenfeld A. Face recognition: A literature survey. ACM Computing Survey. 2003; 35:399–459.
3. Prior FW, Brunsden B, Hildebolt C, Nolan TS, Pringle M, Vaishnavi SN, Larson-Prior LJ. Facial recognition from volume rendered magnetic resonance imaging data. IEEE *Transactions* on *Information Technology* in Biomedicine. 2009 Jan; 13(1):5–9.
4. Ayoob MR. Kumar RMS. Face recognition using symmetric local graph structure. Indian Journal of Science and Technology. 2015 Sep; 8(24).
5. Buddharaju P, Pavlidis IT, Tsiamyrtzis P, Bazakos M. Physiology based face recognition in the thermal infrared spectrum. IEEE *Transactions on Pattern Analysis and Machine Intelligence.* 2007 Apr; 29(4):613–26.
6. Im SK, Choi HS, Kim SW. A direction-based vascular pattern extraction algorithm for hand vascular pattern verification. Etri Journal. 2003; 25:101–8.
7. Nhan BR, Chau T. Classifying affective states using thermal infra red imaging of the human face. IEEE Transactions on Biomedical Engineering. 2010 Apr; 57(4):979–87.
8. Chen X, Flynn PJ, Bowyer KW. Visible light and infrared face recognition. Proc ACM Workshop Multimodal User Authentication; 2003 Dec. p. 48–55.
9. Gundimada S, Asari VK. Facial recognition using multisensory images based on localized kernel eigen spaces.

IEEE Transactions on Image Processing. 2009 Jun; 18(6):1314–25.

10. Flynn PJ, Bowyer KW, Phillips PJ. Assessment of time dependency in face recognition: An initial study. Proc Audio- and Video-based Biometric Person Authentication; 2003. p. 44–51.
11. Guzman AM, Goryawala M, Wang J, Barreto A, Andrian J, Rishe N, Adjouadi M. Thermal imaging as a biometrics approach to facial signature authentication. IEEE Journal of Biomedical and Health Informatics. 2013 Jan; 17(1):214–22.
12. Adini Y, Moses Y, Ullman S. Face recognition: The problem of compensating for changes in illumination direction. IEEE *Transactions on Pattern Analysis and Machine Intelligence*. 1997 Jul; 19(7):721–32.
13. Jenkinson M, Smith S. A global optimisation method for robust affine registration of brain images. Medical Image Analysis, Elsevier. 2001; 5:143–56.
14. Jenkinson M, Bannister P, Brady M, Smith S. Improved optimization for the robust and accurate linear registration and motion correction of brain images. Elsevier, NeuroImage. 2002; 17:825–41.
15. Khader M, Ben Hamza A. Non rigid image registration using anentropic similarity. IEEE *Transactions* on *Information Technology* in Biomedicine. 2011 Sep; 15(5):681–90.
16. Van Soest G, Bosch JG, Van der Steen AFW. Azimuthal registration of image sequences affected by non uniform rotation distortion. IEEE *Transactions* on *Information Technology* in Biomedicine. 2008 May; 12(3):348–55.
17. Viola P, Wells WM. Alignment by maximization of mutual information. Journal of Computer Vision. 1997; 24(2):137–54.
18. Wells WM, Viola P, Atsumini H, Nakajima S, Kikinis R. Multimodal volume registration by maximization of mutual information. Medical Image Analysis. Elsevier. 1996; 1(1):35–51.
19. Zheng JA, Tian J, Deng KX, Dai XQ, Zhang X, Xu M. Salient feature region: A new method for retinal image registration. IEEE *Transactions* on *Information Technology* in Biomedicine. 2011 Mar; 15(2):221–32.
20. Goryawala M, Guillen MR, Gulec S, Barot T, Suthar R, Bhatt R, McGoron A, Adjouadi M. A new 3D liver segmentation method with parallel computing for selective internal radiation therapy. IEEE *Transactions* on *Information Technology* in Biomedicine. 2012 Jan; 16(1):62–9.
21. Lankton S, Tannenbaum A. Localizing region-based active contours. IEEE Transactions on Image Processing. 2008 Nov; 17(11):2029–39.
22. Li H, Yezzi A. Local or global minima: Flexible dual-front active contours. IEEE *Transactions on Pattern Analysis and Machine Intelligence*. 2007 Jan; 29(1):1–14.
23. Perona P, Malik J. Scale-space and edge-detection using anisotropic diffusion. IEEE *Transactions on Pattern Analysis and Machine Intelligence*. 1990 Jul; 12(7):629–39.
24. Jones BF, Plassmann P. Digital infrared thermal imaging of human skin. IEEE Engineering in Medicine and Biology Magazine. 2002 Dec; 21(6):41–8.
25. Candocia F, Adjouadi M. A similarity measure for stereo feature matching. IEEE Transactions on Image Processing. 1997 Oct; 6(10):1460–4.